Design and test of a new two-stage control scheme for SMES-battery hybrid energy storage systems for microgrid applications

Qixing Sun[a,c], Dong Xing[a], Hamoud Alafnan[a], Xiaoze Pei[a], Min Zhang[b] and Weijia Yuan[b*]

a. Department of Electronic and Electrical Engineering, University of Bath, Bath, United Kingdom

b. Department of Electronic and Electrical Engineering, University of Strathclyde, Glasgow, United Kingdom

c. State Grid Energy Research Institute Co.,Ltd, Changping district, Beijing, China

Abstract:

This paper proposes a novel control scheme for a hybrid energy storage system (HESS) for microgrid applications. The proposed two-stage control method is used to control the HESS to stabilize a microgrid's voltage level and extend battery service lifetime during the coupling/decoupling of a microgrid from the main power grid. The conventional HESS control method (the filtration method) is not suitable to compensate for a microgrid's power demand when it is decoupled from the main grid. This research focuses on using a superconducting magnetic energy storage (SMES) and battery HESS to assist with the microgrid coupling/decoupling process. To compensate for the instantaneous high power demand during decoupling, the battery will need to rapidly discharge. Moreover, batteries have difficulty supporting high discharging rates, which results in ineffective compensation of the power demand. In this paper, the high power density of the SMES system combined with the high energy density of a battery shows good performance on stabilizing microgrid bus voltage during the decoupling process. A novel energy management method for the HESS is proposed to improve the battery performance when the microgird coupled/decoupled from main grid. The sizing design is simplified based on the control methodology. Moreover, a SMES and battery HESS experimental platform is built to validate the proposed control methodology and its reliability.

Keywords: Microgrid; Hybrid energy storage system; Superconducting magnetic energy storage; Battery; DC power system.

Highlights:

- This paper presents the solution for the HESS applied in a microgrid system.
- Experimental testing has been conducted to validate the HESS in a microgrid system.
- A new energy management method for the HESS has been established.
- The performance of the preceding control and new proposed control methods are compared.

1. Introduction:

The number of microgrids installed in the main AC power system is increasing and therefore, microgrid security is becoming more important. The microgrid concept is gaining popularity to electrify remote areas and support the energy to islands [1, 2, 3]. In a microgrid system, the energy storage devices are integrated into the system to compensate for the load power demand when disconnected from the main grid. If only a battery energy storage system (BESS) is applied in a system, then when the microgrid is disconnected from the main grid, the instantly increasing power demand from the BESS will accelerate the battery's lifetime attenuation. Therefore, the superconducting magnetic energy storage (SMES) system is proposed to be integrated into a system to build a SMES-battery hybrid energy storage system (HESS) due to the benefits that the SMES system has a short response time and high power output capacity.

A microgrid decoupling process is the conversion of the microgrid from grid connected mode to islanded mode. Previous researchers [4] have studied the SMES-battery HESS applied in microgrids to deal with long-term power demand fluctuations of a microgrid in islanded mode. The energy storage system implemented in a microgrid has been studied in previous studies [2, 5, 6], with most of these studies focusing on the energy storage system dealing with long-term fluctuating power demands. To date, for the authors' best knowledge, there are no published papers focusing on the microgrid decoupling response process of a HESS when a microgrid disconnects from the main grid. When a microgrid is decoupled, the energy storage

devices need to support the load demand in the microgrid. Therefore, the energy storage system needs to provide instantaneous high power when the main grid is disconnected from the microgrid.

A BESS has the advantages of high energy density, high efficiency, high robustness and high energy capability to deal with long duration power demands, which makes it one of the most popular energy storage devices to be applied in the microgrid [7, 8, 9]. The lead-acid battery is typically the most suitable choice to apply in a power system due to its low cost and technical maturity. However, the lead-acid battery has a low power density and low discharging rate, which results in requiring more sets of lead-acid batteries applied in the microgrid to deal with fast-changing power demands such as voltage drops in the power system.

Energy storage devices will have an instantaneous high amount of power demand from a microgrid when it disconnects from the main grid. However, a lead-acid battery is not capable of responding to the high transient power demand [10, 11] and high discharging rate, which can also accelerate batteries attenuation [12, 13]. One solution for utilizing a battery in a microgrid decoupling process is to use a large number of lead-acid battery sets, to enable each battery set to have a small amount of power output and discharging rate. However, the large amount of batteries will increase maintenance costs. To solve this problem, hybridizing a high power density energy storage device with a battery is proposed. Several researchers have studied the application of a supercapacitor with a lead-acid battery in a the power system [14] and electric-vehicle [15]. J Li studied a SMES and battery HESS applied in the AC power system to deal with frequency regulation [4]. Compared to the supercapacitor and other high power density energy storage devices, a SMES system has the advantages of higher power density [16], low self-discharge rate [17] and higher peak current handling capability [18].

The cost of SMES systems is dramatically reducing with the development in materials research [19, 20]. Some studies show the positive side of the cost-benefit analysis of SMES systems [21, 22]. SMES-battery HESS have also been proposed to deal with the high fluctuating demands for an electric bus [23]. H Alafnan [24] proposed to use a SMES-battery system in an all-electric ship. SMES and battery HESS have also been applied to smooth renewable power generation output [25], AC system primary frequency control [26] and to balance the power demand between the generation part and load [27], etc. However, no literature has been found that applies a HESS in a DC microgrid decoupling process. Furthermore, no experimental work of a SMES-battery HESS has been conducted to prove the achievability of a SMES-battery HESS. One of the crucial points is that a DC network needs a more accurate energy management control method to deal with the power sharing from different energy storage systems. In this paper, a SMES-battery HESS is proposed to deal with the microgrid decoupling process. The high-power density device—SMES system—is used to deal with the instantaneous high power demand when the main grid is not able to support the power to the DC microgrid, which results in the battery power output having a lower discharging rate, hence, extending the battery lifetime. Therefore, it is technically and environmentally friendly to build a SMES-battery HESS.

A semi-active control topology and an active control topology are proposed to control the proposed SMES-battery HESS. The semi-active control circuit has the advantages of less electrical components used and low energy losses. This circuit structure has been proposed for supercapacitor/battery HESS control [28, 29] and SMES-battery HESS control [30]. However, the semi-active control topology makes the battery power output uncontrollable. Therefore, to achieve a more advanced control of the proposed hybridized system, the active control topology is selected for the proposed SMES-battery HESS. The active control topology uses an additional DC/DC converter for the battery compared to the semi-active topology, which makes the battery power output more controllable. In this paper, one novel point is that a real SMES system in the SMES-battery HESS is firstly used to test the system reliability and achievability. AM Gee [31] has done the experimental work using a normal copper inductor with battery to represent the SMES-battery HESS in an AC system. However, in the experiments, it was found that the copper inductor is incapable of representing the SMES system in the power system. The copper inductor has high ohmic losses and also added high noises in the AC power system. Moreover, the ohmic losses also decreased the energy capacity of the copper inductor.

The control method for the HESS is more complicated because of the different energy storage systems having their own unique features. Therefore, the control method should take the advantages of their features into account to make the HESS work more effectively. There are many power control methods proposed in the literature. Fuzzy logic control, which the control method design based on human knowledge and experiences to achieve the purpose of the control. The fuzzy logic control for the HESS using a nonlinear system without a precise mathematical model to achieve highly suitable control to coordinate the various energy storage devices. The fuzzy logic control method has been previously proposed for railway power systems [30] and wind power applications [32, 33]. These literature show the benefits of protecting the battery from a fluctuating power demand. However, the control algorithm of the fuzzy logic controller is selected empirically, which is not suitable for a new system. Furthermore, the design process of the fuzzy logic controller is convoluted. Filtration method, which uses frequency filter to identify the large fluctuations power demand and slow-changes power demand from the HESS power demand. Fast responding energy storage devices such as SMES systems and supercapacitors are used to deal with high fluctuating demands and the battery is used to compensate long-term and low-frequency power demands. The filtration method has good results when applied to PV systems [34], microgrids [35] and EVs [36]. The filtration method is one feasible control method for the HESS because it can control the fast responding energy storage device to compensate for the power demand at the very beginning and let the battery slowly discharge to meet the power demand. However, it has difficulty for the system sizing design and the cut-off frequency design. A. Allègre [37] proposed to use a real-time data-driven control of

the supercapacitor/ battery HESS, which can achieve a high utilization factor of the supercapacitor by suspending the battery activation until the energy in the supercapacitor reaches a threshold. However, the real-time data-driven control method may damage the supercapacitor when it is fully discharged. The power grading control has been proposed to use for electric vehicles [38]. The grading control method manually classifies the power demand for different conditions and uses different energy storage devices to deal with the classified power demand. This control method highly depends on the specific implementation. B. Hredzak [39] proposed to use the model predictive control method for a HESS, to reduce the battery maximum power demand and compensate with the low efficiency of the fast responding energy storage device in return.

Droop control is able to take advantage of different kinds of power sources to manage the power output to meet the power demand from the power system. J. Li [25] and AM. Gee [31] have proposed to use droop control for HESS control. However, a droop controller is a linear controller. Droop control can deal with various voltage fluctuations for a HESS applied in the power system. However, it has difficulty in designing the SMES system power output droop factor and battery power output droop factor. Moreover, a droop controller cannot work correctly when a power system has slightly changed such as add/remove some loads/generation parts because the power output has a linear relationship with the HESS power demand. The existing HESS control methods are not suited to deal with a microgrid decoupling from the main AC grid due to less consideration of the huge amount of instant increasing power demand and also the battery maximum discharging current limitation. The previous methods are designed for small power fluctuations but not for high instantaneous power demand increases such as voltage droop in the power system.

In this paper, a new control method combining Proportional-Integral (PI) control and droop control for the SMES-battery HESS is proposed. The proposed control method has the advantages of better performance of the battery power output and is more reliable when the load changes. The proposed control method uses the energy remaining in the fast-response energy storage device (SMES) as the reference factor of the battery droop controller. This can make the battery power output smoother. By combining PI control in the system, it can make the system works in any situation. Two different stages of discharging will be applied in different circumstance to compensate for the power demand, which will be discussed in the following section. Moreover, taking the energy remaining in the fast-responding device as the reference parameter of the battery controller can make the control method much simpler and easier to design. Moreover, the control method of the charge state and standby state are modified for the voltage droop application and verified by the experimental platform.

The extension of the battery service lifetime is one of the significant advantages of the HESS. Y. Cui [40] showed that rapid charging/discharging will reduce battery service lifetime. R. Xiong's [41] showed that high discharging rates can result in a dramatic reduction in battery service lifetime. The study of S. Panchal [42] showed that batteries are difficult to accomplish high energy density, which means that battery only energy storage systems have a difficulty to deal with sudden power changes such a microgrid decoupling from the main AC grid. For the microgrid decoupling process, it can be considered that the power demand from the HESS is fixed. To extend battery cycle time and reduce the BESS size in the SMES-battery HESS, decreasing the battery discharging rate and using the SMES to deal with the instant power demand when the microgrid is disconnected, is one of the best options.

In this study, the experimental platform of the SMES and battery storage system has been built to simulate the HESS in a microgrid. Furthermore, the proposed control method is applied in the HESS. Moreover, based on the experimental results, the control method of the SMES charge and standby states has been modified when compared to the conventional control method [43]. The experimental setup and control methodology changes will be discussed in sections 5 and 6.

2. System description and control of the HESS:

2.1 System description:

Fig. 1 shows the system configuration of the proposed DC microgrid with renewable generations and AC loads in the power system. A bidirectional grid interface converter is used to control the microgrid connection/disconnection from the main AC grid. The power generation systems such as PV generation, wind power generation and fossil fuel generation are connected to the DC transmission lines. The SMES system and the battery HESS are used to stabilize the voltage on the distribution side. The active control topology is applied to the HESS system. A bidirectional DC/DC converter is used to control the BESS charge and discharge cycles. The DC chopper is designed to support the power exchange between a SMES system and the DC microgrid. The proposed topology has the advantages of less electrical components used and the charging/discharging process is controllable for the DC network.

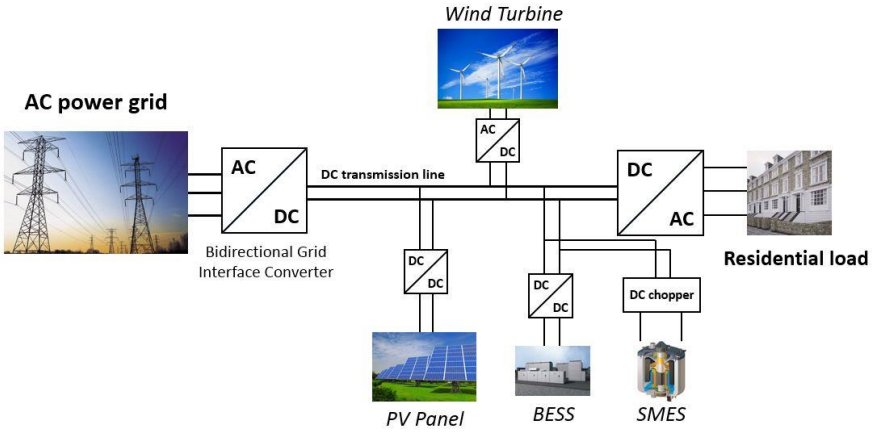

Fig. 1. DC system with SMES-battery HESS.

2.2 DC/DC converter for the battery packs

A bidirectional DC/DC converter is capable of tracking capacity, has robust performance and also high efficiency [44, 45]. The battery DC/DC converter is shown in Fig. 2. In this paper, two control mechanisms are applied to the bi-directional converter under different circumstances, which will be discussed in section 3. The theory of two control mechanisms is described in subsection 2.2.

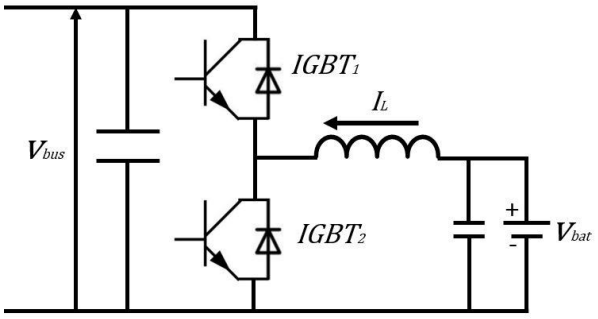

Fig. 2. Battery DC/DC converter.

2.2.1 Boost mode for the bi-directional converter:

Boost mode is the basic mode for a DC/DC converter. In boost mode, the controller controls the thyristor in the converter to achieve the required voltage output. Boost mode controls the duty cycle of IGBT 2 in Fig. 2, to stabilize the output voltage. The relationship of the DC/DC converter output voltage V_{out} with the duty cycle of IGBT 2 D_{IGBT2} is described by:

$$V_{out} = \frac{1}{1-D_{IGBT2}} \cdot V_{bat} \quad (1)$$

Boost mode is able to stabilize the output voltage regardless of the external circuit configuration, which is good for voltage regulation control of the BESS. However, the boost model is not able to control the battery performance when the output power is rising.

2.2 Conventional SMES control method:

The DC chopper is designed to control the SMES magnet, which is used to store energy. The three operating states are: charge mode, discharge mode and standby mode. Charge mode and discharge mode are used to exchange power between the SMES system and the main AC grid. The standby mode is used to maintain the energy in the SMES magnet. The three operation modes are described in the following subsections:

2.2.1 Charge mode:

The charge mode only works when the controller requests the SMES system to absorb energy. In this situation, the current path in the SMES system is shown in Fig. 3. In this mode, IGBT 3 and IGBT 4 are constantly on to charge the SMES system from the DC bus.

Applying Kirchhoff's voltage law (KVL), the SMES system charge state can be represented as:

$$U - L\frac{dI(t)}{dt} - I(t)R_l = 0 \tag{2}$$

where U is the DC bus voltage; L is the inductance of the SMES magnet; R_l is the equivalent self-resistance of the SMES magnet (which is mainly caused by the resistance of the power junctions in the SMES magnet); $I(t)$ is the current in the SMES magnet at time t; and, t is the time duration for the SMES discharge from the current I_o;

Assuming that the initial current in the SMES magnet is I_o, the instantaneous current in the SMES magnet can be represented by:

$$I(t) = I_o \exp\left(-\frac{R_l tD}{L}\right) + \frac{U}{R_l}\left[1 - exp\left(-\frac{R_l tD}{L}\right)\right] \tag{3}$$

where D is the duty ratio of IGBT1 in the SMES chopper. In this study, the inner resistance of the SMES magnet is neglected, which means $R_l \approx 0$. Therefore, (3) can be simplified to:

$$I(t) = \frac{U}{L} t * D + I_o \tag{4}$$

The power stored in the SMES system can be calculated by:

$$E(t) = \frac{1}{2} L I^2(t) \tag{5}$$

2.2.2 Discharge mode

The current flow for the discharge mode is shown in Fig. 3. For discharge mode, IGBT 3 is off and the controller controls the duty cycle of IGBT 4 to achieve the desired output current I_{ref}.

For discharge mode, applying KVL to analyse the SMES discharge process yields:

$$-L\frac{dI(t)}{dt} + I(t)R_l + I(t)R = 0 \tag{6}$$

Assuming the initial current in the SMES is I_o, the current in the SMES at time t can be represented as:

$$I(t) = I_0 \exp[-\frac{(R+R_l)t}{L}] \tag{7}$$

Therefore, when the duty ratio for IGBT 4 is D, (7) can be simplified as:

$$I(t) = I_0 \exp - \frac{R*t*D}{L} \tag{8}$$

The SMES power output can be represented as:

$$P_{SMES}(t) = \frac{dE_{SMES}(t)}{dt} = \frac{d0.5*I^2(t)*L}{dt} \tag{9}$$

As it can be seen from (9), the relationship between the SMES system discharge duty ratio and SMES system output power are not linear. During this work, PI control was used to control the IGBTs for the SMES system discharge cycle.

2.2.3 Standby mode

When the SMES system does not need to exchange power from the main AC grid, the chopper needs to operate in standby mode to keep the power stored in the SMES system. Due to a particular feature of the SMES system, the chopper needs to frame an electrical closed loop to keep the current flowing in the SMES magnet. The current path for standby mode is shown in Fig. 3, which only requires IGBT 3 to be held constantly off and IGBT 4 to be held constantly on.

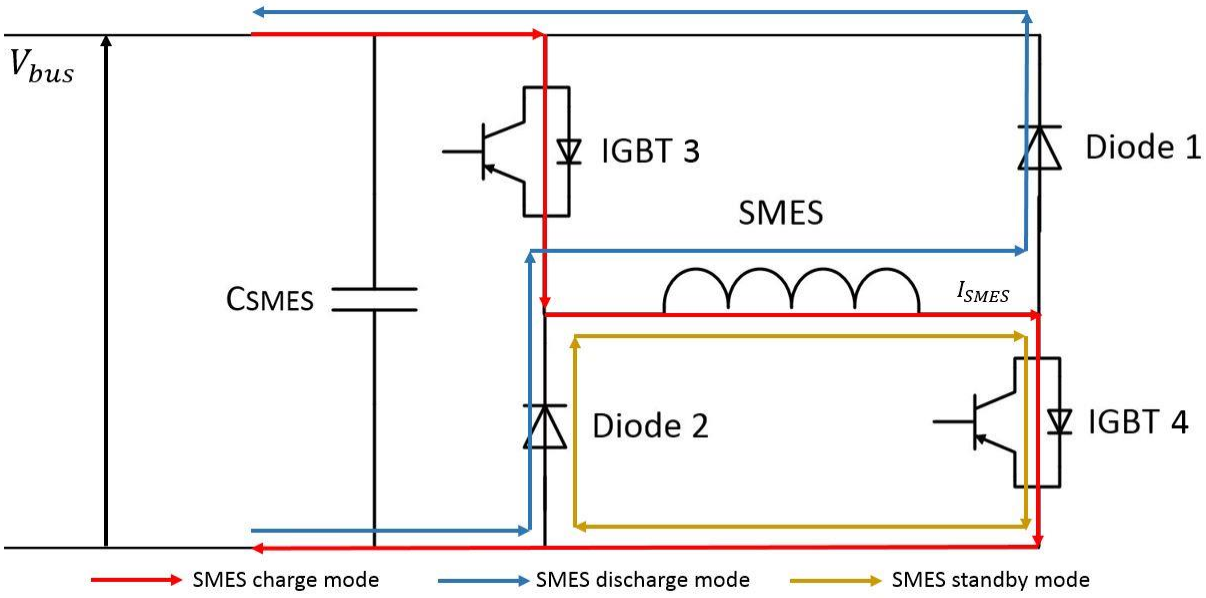

Fig. 3. The SMES chopper current paths.

2.3 Filtration method

The conventional filtration method for the HESS control [46, 47] is shown in Fig. 4. In the filtration method, the power demand of the power system is dealt by the low pass filter. The low frequency power fluctuation is dealt with by the battery in the HESS and the rest of the power is dealt by the fast responding energy storage devices (such as the SMES and supercapacitor). In this case, the battery has slow charge/discharge power changes and lets the SMES deal with the high fluctuating power demand. The slow battery output changes are beneficial to extend the battery service lifetime. The filtration method has the advantages of extending battery service lifetime by reducing the battery charge/discharge cycle from a high fluctuating power demand. However, the sizing design and the cut-off frequency for the filtration method is difficult to obtain.

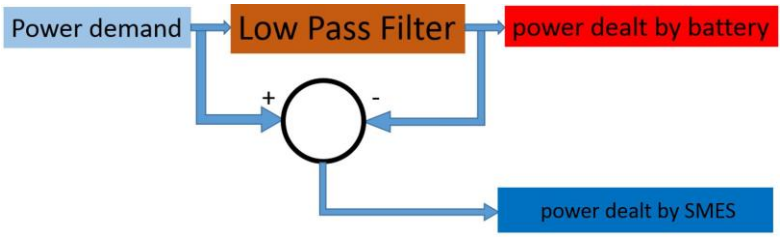

Fig. 4. The filtration method.

3. Novel control methodology for the HESS to deal with a microgrid decoupling process

Compared with previous research, which uses the SMES-battery HESS to deal with fluctuating power demand [33, 48, 49] (the fluctuation is 0% to 10% of the system total power demand), the microgrid decoupling process has a much higher power demand in a very short period of time (the demand is 100% of the system total power demand). Therefore, the HESS control methodology for a microgrid decoupling process will be different from the previous researchers' solutions. The energy management rules of two different energy storage systems are the most crucial part for the HESS control. An appropriate energy management method will not only keep the power system stable but also extend the service lifetime of the HESS. The new proposed method has the advantages of the SMES quick response time, high power density and long service lifetime. The battery sets have high energy density and low economic cost. Because the size of the distribution network may change, a novel two-stage control method for the HESS, to keep the system stable and extend the battery service lifetime, is proposed. Moreover, the new proposed control method considers the features of battery charge/discharge relevancy with battery service lifetime.

The flow diagram of the proposed two-stage control method is shown in Fig. 5. When a microgrid is connected to the main AC grid, the controller controls the SMES and the battery sets to charge them to their rated energy capacities, and then

switch to HESS standby mode. When the microgrid disconnects from the main AC grid, the controller operates in stage one, where the SMES and battery sets deal with the microgrid decoupling process. In this stage, the SMES is used to deal with the instant power demand from the microgrid and the battery slowly increases its power output. This method aims to decrease the battery discharging rate when the microgrid disconnects from the main AC grid. When the SMES is fully discharged and stage one cannot sufficiently compensate for the power demand from the microgrid, which can potentially be caused by load power demand changes, stage two of the proposed control method starts functioning.

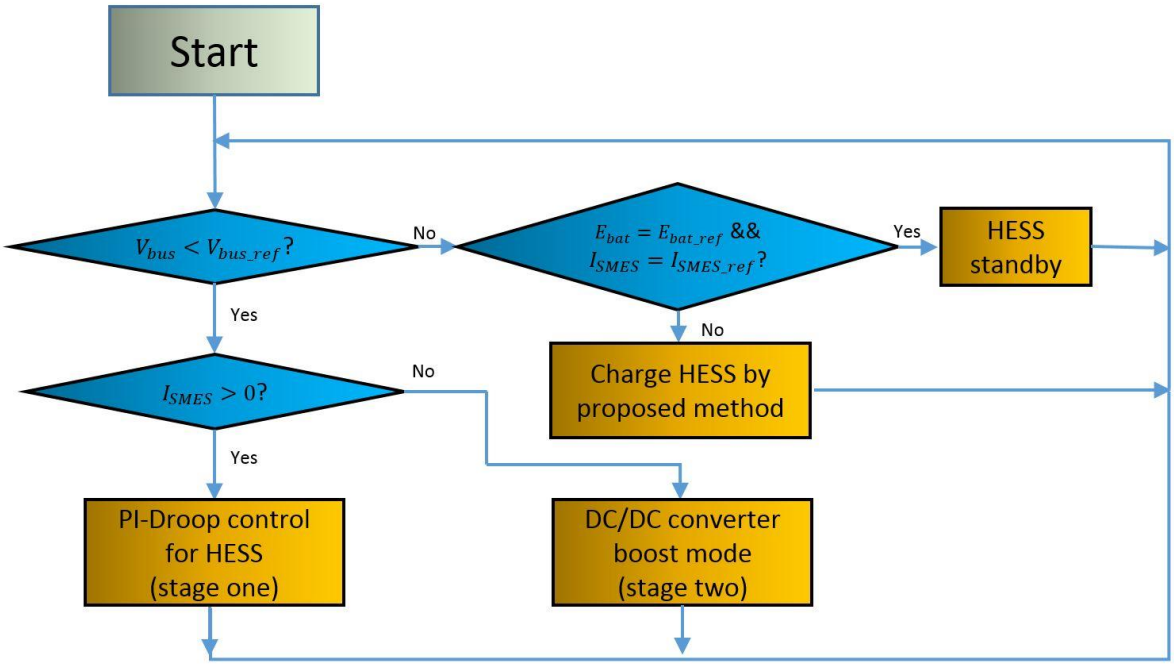

Fig. 5. The proposed control method for voltage droop application.

3.1 HESS charge state control methodology

In previous SMES-battery HESS research, most solutions charge the HESS with unfixed input power such as using a PI controller [48], droop controller [4] and the filtration method [50] to charge the HESS. However, in experiments, it was found that charging the HESS using unfixed power can cause a voltage fluctuation on a DC power system. The HESS acts as one high-power load in the power system when the HESS is charging. During charge mode, the control method charges the HESS with different charging power, which increases the load demand fluctuations, which results in more instability in the system. To keep the power system stable and to enhance the robustness of the HESS, the power demand for the HESS should be consistent. Therefore, is it proposed to charge the SMES and battery energy storage system at a fixed power for this voltage droop application.

3.2 Two-stage discharge control method

The new proposed control method is applied when the microgrid disconnects from the main AC grid. Reduction of the discharging rate for the battery sets is one of the advantages of the proposed control method. Moreover, in previous research, no study has been conducted to combine PI control and droop control for a SMES-battery HESS. The control method has two stages and each stage has a different purpose for the HESS, to compensate for the microgrid power demand. Stage one operates when the microgrid disconnects and the main purpose for stage one is not only to compensate for the voltage drop but also to extend battery service lifetime. Stage two is used when stage one cannot stabilize the voltage in the power system to the rated level. Stage two starts to operate only when the maximum load demand in the power system changes due to newly added loads in the power system.

3.3 New proposed PI-droop control method for the SMES-battery HESS

The coordination for the SMES and battery power input/output is the main focus of this research. Based on battery lifetime research, a low discharging rate can be used to increase battery service lifetime [51]. In real applications, the power demand requires fast response from the energy storage system. Therefore, the ideal situation is to use the SMES to deal with the fast-changing power demand and for the battery sets to slowly change their power output. During stage one, the SMES is used to stabilize the load voltage and the battery output power is controlled by the energy remaining in the SMES.

In the new proposed control method, stage one is applied when the SMES is not fully discharged. The PI controller is used to control the SMES to deal with the power demand. The reference parameter for the $\mathrm{PI_{SMES}}$ controller is the DC bus voltage. The battery output power keeps increasing due to the energy remaining in the SMES decreasing and the SMES deals with the remaining power demand for the HESS, to compensate for the load power from the microgrid. This makes the proposed control system have the advantages of low complexity and prevents the battery sets from a surge increasing the discharging rate. For the SMES and battery HESS, either only using PI control or only droop control needs a complex calculation to design the controller. In the new proposed control method, the controller design is much easier due to the combination of PI control with droop control. The control scheme of the stage one control methodology in the two-stage controller is shown in Fig. 6.

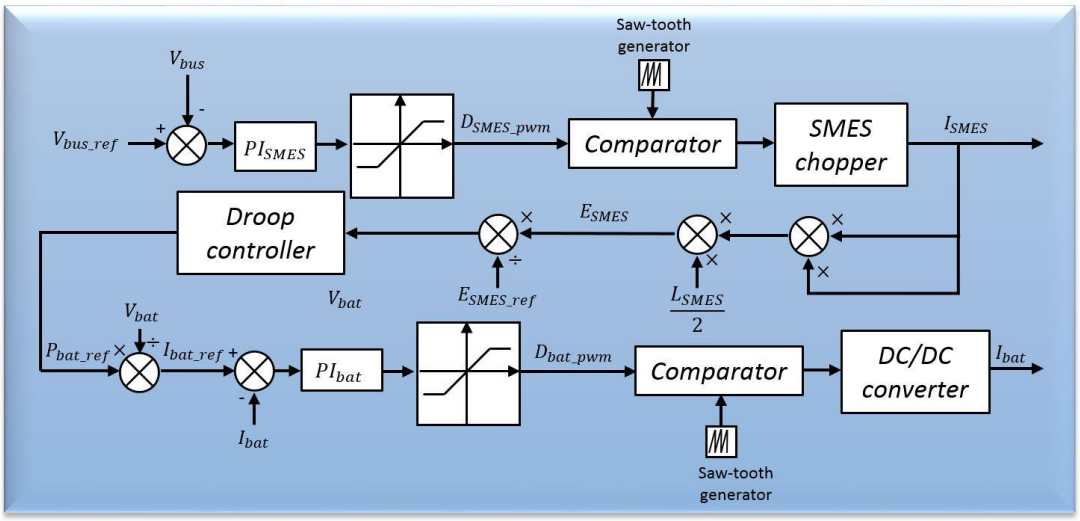

Fig. 6. Stage one control methodology.

The droop control principle for the battery control is shown in Fig. 7. The battery power output can be calculated as:

$$P_{bat\_out} = k \cdot \frac{E_{smes\_max} - E_{smes}}{E_{smes\_max}} \tag{10}$$

where E_{smes_max} is the SMES rated energy capacity; E_{smes} is the energy remaining in the SMES; k is the droop coefficient of the droop controller; and, P_{bat_out} is the battery output power.

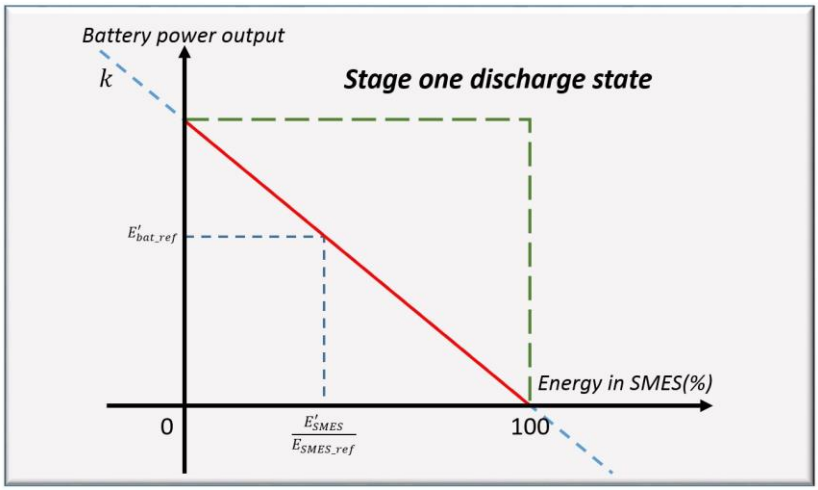

Fig. 7. Droop controller design.

The battery output power is related to the energy remaining in the SMES. To achieve the energy allocation method, I_{bat_ref} can be calculated using (1). The DC/DC converter is used to control the battery output current. When the SMES is not fully discharged, the energy management control method for the battery is droop control. The reference parameter for the battery droop controller is the ratio of the energy remaining in the SMES (E_{SMES}/E_{SMES_ref}).

Stage two operates only when the SMES is fully discharged and the battery power output during stage one cannot compensate for the microgrid power demand. During stage two, the bidirectional DC/DC converter for the battery sets is using boost mode to stabilize the load voltage. This can ensure that the HESS is able to stabilize the power system. Stage two can guarantee the system robustness when the load changes or the previous droop control coefficient cannot fix the new system, which means the load/generation size in the power system changes.

The new control method first proposes to use PI control combined with droop control for the battery-SMES HESS. Moreover, this study is the first research conducted to date using the energy remaining in the SMES, as the battery output reference. Due to the energy stored in the SMES, which has the exponential relationship with SMES current, applying the energy remaining in the SMES as the battery control reference can make the battery discharging rate stable. This can be utilized to extend the battery service lifetime. PI control is used for the SMES to stabilize the voltage drop and secure the system stability in different circumstances.

3.4 Battery discharging rate design

The battery manufacturers normally provide an optimal discharge rate for their batteries. The over-range discharging current will accelerate the degradation process of batteries. Therefore, for the droop controller, the maximum output current I_{out_max} for each battery should be less than their maximum output current limitation I_{out_lim}:

$$I_{out\_max} \leq I_{out\_lim} \tag{11}$$

In the proposed HESS system, the battery energy storage system should be able to provide enough power to the load when a voltage drop occurs. The maximum power consumption P_{load_max} is determined by the power system configuration. The battery energy storage maximum power output P_{bat_max} can be calculated by:

$$P_{bat\_max} = V_{bat} \cdot I_{out\_max} \geq P_{load\_max} \tag{12}$$

The SMES can coordinate with the battery to stabilize the load voltage and therefore achieve a high reliability for the proposed method. By considering the energy in the HESS, the selected battery minimum discharging rate k for the battery output power is designed as:

$$k \geq \frac{P_{load\_max}^2}{2 \cdot E_{smes\_max}} \tag{13}$$

4. Sizing study for SMES and battery:

In the SMES and battery HESS study, the energy storage system size of the SMES and battery should be able to deal with the instantaneous increasing power demand when a voltage drop occurs and also long-term power demand for the HESS to support the power system. Due to the new proposed control algorithm, the sizing study is different from the previous HESS sizing research [29, 38, 45, 52]. The new proposed sizing design method has the advantage of less complexity and also guarantees system reliability due to the two-stage control methodology.

The sizing study is one of the most difficult parts of HESS research. An oversized design of the HESS will increase the cost of the system and insufficient power/energy capacity can cause the HESS not to be capable of meeting the power demand from the system. The SMES and battery HESS should be able to meet both the energy requirements and power requirements from the power system. Therefore, there will be three specifications for the SMES-battery HESS sizing study:

i). SMES maximum output power P_{smes_max} should be larger than the maximum power demand from the power system P_{system_max}:

$$P_{smes\_max} > P_{system\_max} \tag{14}$$

ii). The battery energy capacity should be able to meet the load energy demand.

iii). The energy capacity of the SMES should be able to compensate for the energy demand before the battery output power can meet the power demand.

In a HESS dealing with a microgrid decupling process, the battery energy capacity is designed by the maximum power demand of the distribution network P_{system} and the HESS designed compensation time T for the HESS to stabilize the distribution

network voltage. The SMES energy capacity is negligible compared with the battery energy capacity. Therefore, for the battery sizing design, the battery size E_{bat} can be calculated by:

$$E_{bat} \geq P_{system} \cdot T \tag{15}$$

The new proposed method can adequately simplify the SMES sizing design due to the proposed control method. The SMES has been used to relieve the battery power output from the instant increasing power demand.

In the proposed method, the HESS is able to deal with the power demand, since the SMES can handle the power demand before the battery takes over the power output from the SMES. Therefore, the SMES size should be:

$$E_{smes} \geq \int_o^t P_{load}(t)dt - \int_o^t P_{bat}(t)dt \tag{16}$$

Where the battery output power is limited by its designed discharging rate γ [W·s^{-1}]. In this case, the initial power output for the HESS is zero before a voltage drop occurs. The size of an SMES can be calculated by:

$$E_{smes} \geq \int_o^t P_{load}(t)dt - \int_o^t \gamma \cdot tdt \tag{17}$$

The sizing design of the new proposed method using (16) (Battery sizing) and (17) (SMES sizing) is more straightforward compared with other different sizing designs. Once the system sizing and the discharging rate for the battery is defined, the SMES size can be easily calculated.

5. HESS experimental platform description:

To verify the new proposed control method and the HESS control circuit topology, an experimental platform for the SMES and battery HESS applied in a DC power system was built. The SMES has its own feature that other kinds of energy storage systems cannot match such as high power density and long service lifetime. The partnership of the SMES and battery is another critical point of this research.

The experimental test-rig structure is shown in Fig. 8, where the DC power source represents the main grid. The DC power source output represents the microgrid connection and disconnection from the main grid. The HESS control circuit using the active topology, as discussed previously, uses a controller from Texas Instruments (TI) (TMS320F28335) in the experiments. High power resistors are used to represent the load part of the proposed system.

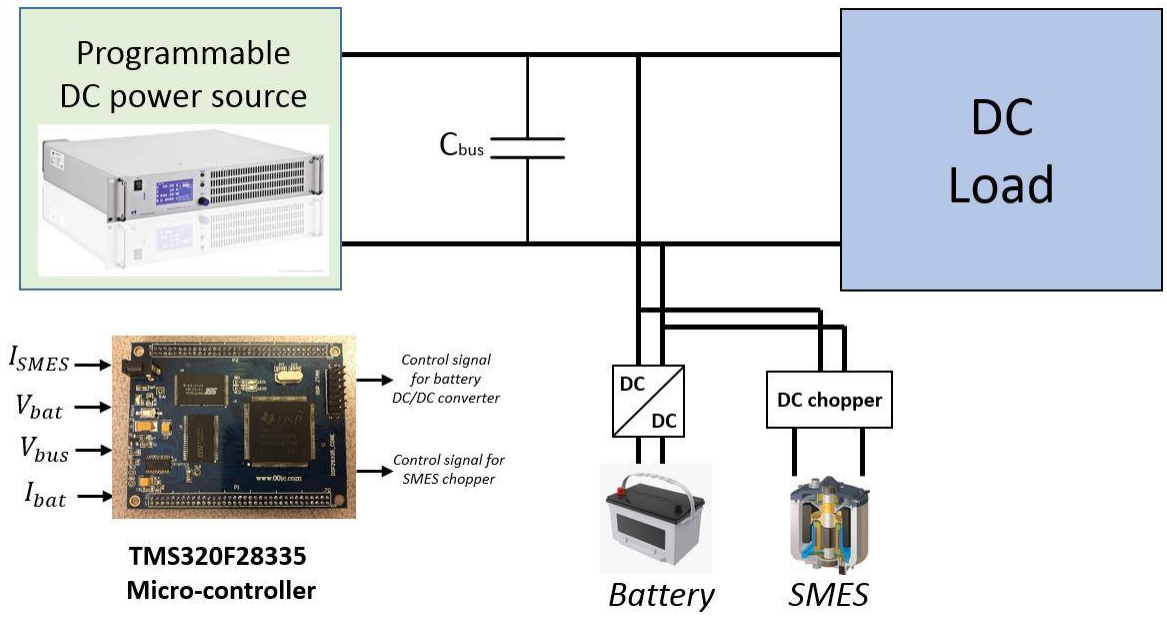

Fig. 8. Laboratory experimental test-rig configuration

Fig. 9 shows the experimental test-rig setup of the SMES and battery HESS applied in a DC network. LAB/SMS5300 is used as a DC power source to represent the main grid. A self-made SMES magnet is used in the HESS and the SMES magnet is dipped into liquid nitrogen. The SMES parameters are shown in the Appendix, Table 2. The critical current for the SMES magnet is 42 A. For the safety reasons and low joule losses, the SMES working current is approximately 80% of the critical current,

which is 33 A. The new proposed control algorithm is implemented in the TMS320F28335 TI micro-controller. The micro-controller is embedded on the control board, which is also used to measure the voltages and currents in the system. The gate drive circuits for the IGBTs are also embedded in this control board. A National Instruments (NI) data acquisition card is used to collect measurement data of the load voltage; SMES current; battery current and battery voltage. A DC current clamp is used to monitor the SMES current. The main grid connection/disconnection from the microgrid is created by the programmable DC power source (LAB/SMS5300).

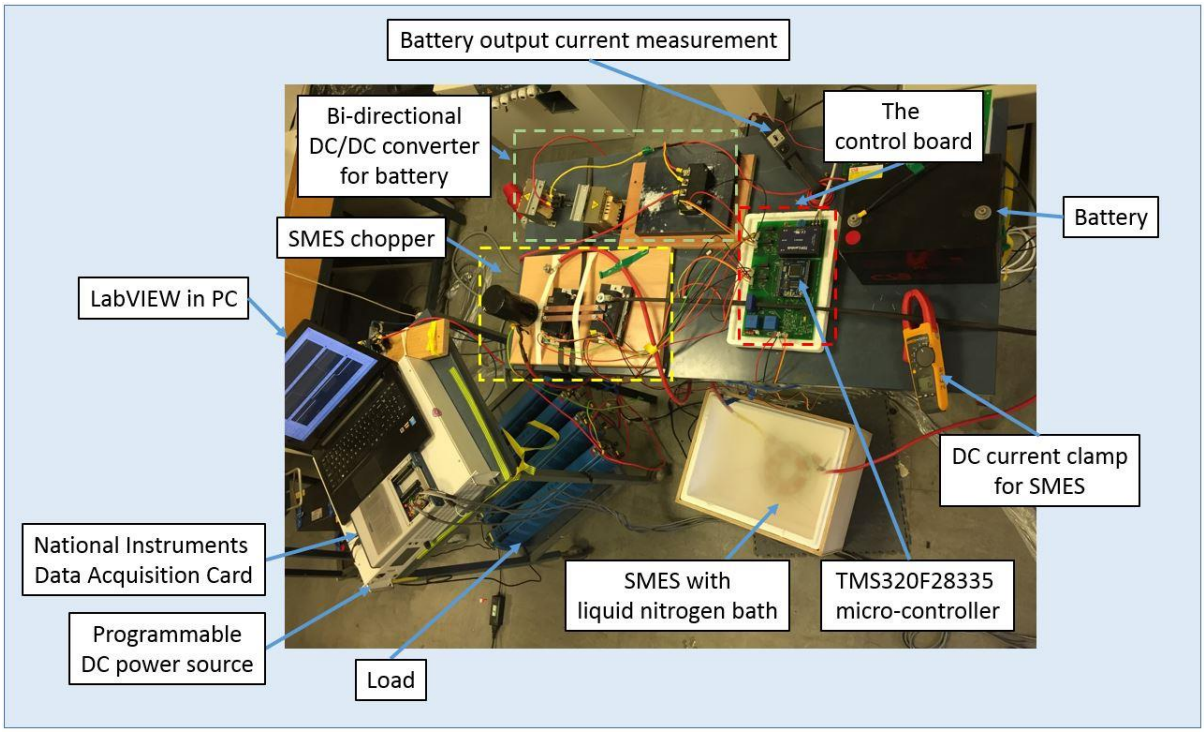

Fig. 9. SMES and battery HESS in DC microgrid experimental test-rig system setup.

The experimental system was used to verify the system reliability and show the performance of the HESS using the new proposed control method. In the experiments, the initial SMES current is zero and the battery is at rated energy capacity. The controller starts to charge the SMES when the DC system voltage is at a predefined value (20 V in this experiment) and keeps the SMES working at rated current (32 A in this experiment). The two-stage control method works to stabilize the load voltage when the microgrid is disconnected from the main grid.

6. Experimental results:

The real-time operation of the experimental HESS aims to test the performance of the SMES-battery HESS system and the new proposed two-stage control algorithm. The experiments are used to test the experimental operation of the proposed control circuit and the control method applied in a lab scale DC system. Power system size simulation results are presented in Section 7 to test the control method performance in the power system. To test the HESS and control algorithm performance, the experimental tests of the SMES-battery HESS starts from being charged by the power system. Then the control method controls the circuit to keep the rated energy stored in the SMES and battery. By applying the two-stage control method, the HESS discharges to stabilize the bus voltage when the microgrid is disconnected from the main grid. This represents a whole cycle of the HESS to deal with the microgrid connection/disconnection from the main grid. In addition, this experiment is able to test the droop coefficient design of the novel control method.

One properly designed droop coefficient of the battery control can make sure the battery can compensate for the system power demand at the time the SMES is fully discharged. To test the performance of the two-stage control method for the HESS, the supply power disconnection from the lab-scale microgrid is created by the LAB/SMS5300 programmable DC power source. The DC power source disconnects from the microgrid at 5.52 s and restores the power supply at 11.52 s. During this time period, the HESS is used to support the load voltage. When the generation part is restored to support the load, the controller controls the SMES chopper to charge the SMES to its rated current and controls the battery bidirectional converter to charge the battery to its rated voltage. During this time, the generation part is able to provide sufficient power to the load, thus the HESS is working in standby mode. From 0 s to 5.52 s and 11.52 s to 15 s, there is no power demand from the power system and the HESS operates in standby mode. Due to the SMES eddy current losses, which are caused by the IGBTs in the SMES chopper, the SMES needs a small amount of energy from the power system to keep the SMES current at the rated

level. This causes a small voltage ripples on the DC bus, which is about 0.2 V in these experiments. However, with increased system capacity, the eddy current losses for the SMES have less impact within the power system. As shown in Fig. 10(a) and Fig. 10(b), when the SMES is fully discharged, the battery output power can fully compensate for the load power demand. This confirms that the successful sizing design is applied to this system and the droop coefficient of the battery droop control is satisfactory. The stable discharging current change is conducive to battery lifetime extension. The appropriate sizing design and droop coefficient design have the ability to prevent the battery output current from experiencing a sudden change.

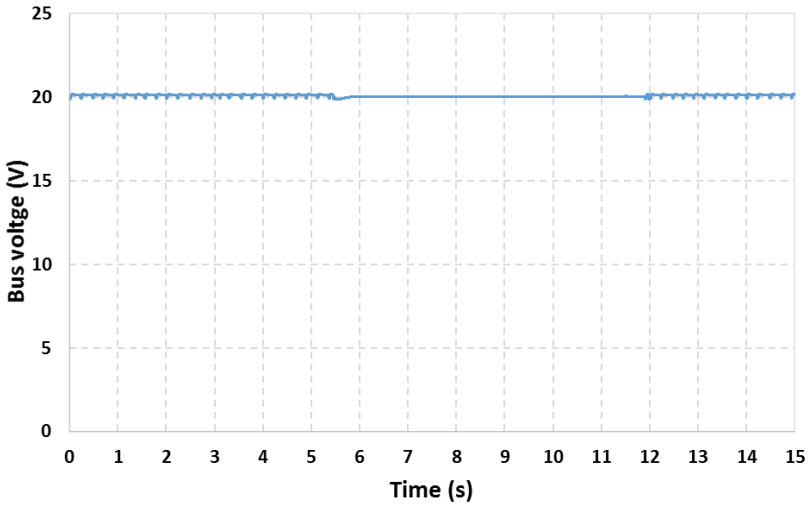

(a)

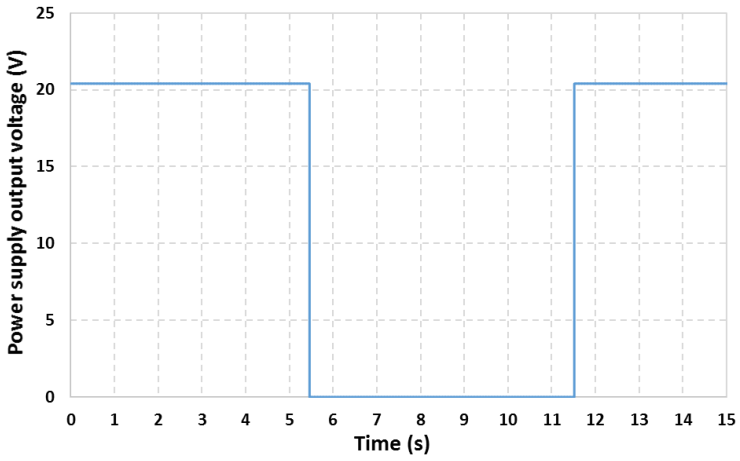

(b)

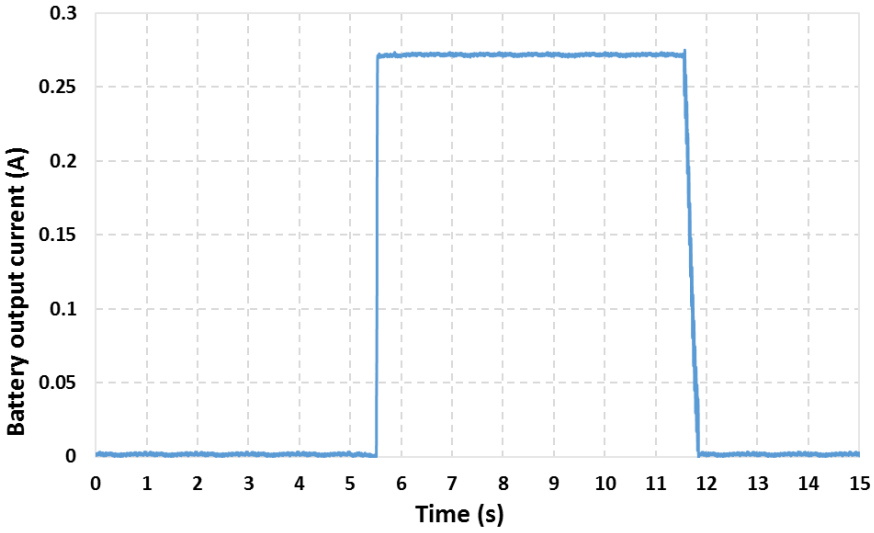

(c)

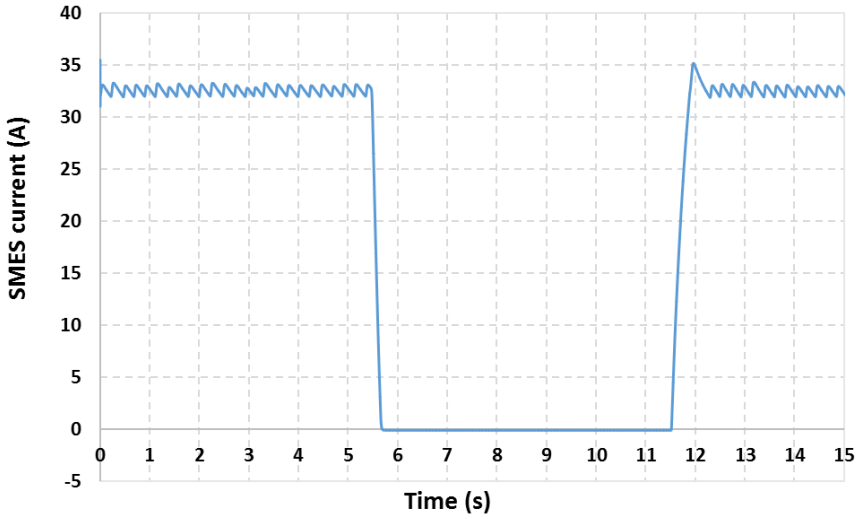

(d)

Fig. 10. Experimental results for the SMES-battery HESS to deal with one microgrid decoupling: (a) microgrid bus voltage (b) main grid support voltage (c) battery output current (d) SMES current.

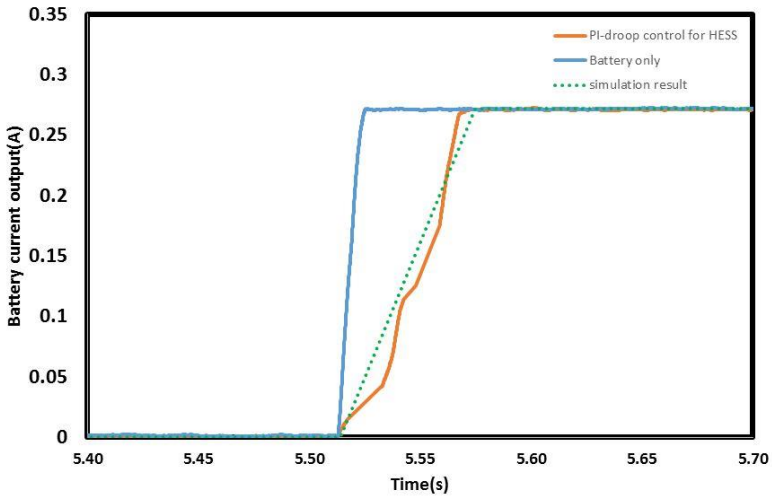

Fig. 11. Experimental results for the PI-droop control HESS and battery only system.

Another experiment was conducted for the battery only system to stabilize the microgrid bus voltage when the microgrid converts to islanded mode. The battery performance to compensate for the power demand during the microgrid decoupling process of the proposed control method applied in the HESS and the battery only system using the DC/DC converter control method are shown in Fig. 11. As can be seen from Fig. 11, the PI-droop control method in the two-stage control decreases the discharging rate and allows the battery to have 0.06 s more time to reach the rated battery output power. This shows the advantages of the proposed two-stage method compared with the battery only system on giving adequate time and decreasing the discharging rate for the battery to respond to the power demand. The simulation result also shown in Fig. 11, the simulation results can match the experimental results which proves the accuracy of the numerical model.

7. Simulation verification:

After the new proposed method experimental verification was achieved, the simulation for the proposed method applied in the power system was conducted to test the performance in the power system. The experimental results show the achievability of the proposed method applied in the system to deal with a microgrid decoupling process. However, the power system scale SMES-battery HESS is not able to be tested in the lab. Therefore, the simulation work is to simulate the proposed HESS control method working in the power system to stabilize the load voltage in a microgrid.

A model of the SMES and battery HESS in a DC network was developed in Matlab/Simulink. In this case, the distribution network power demand was 334 kW. The battery energy storage terminal voltage was 240 V. The designed battery maximum output power changing rate was 56 kW/s. The SMES size can be calculated by (17), which is 0.98 MJ. The bus voltage was 380 V and the microgrid is disconnected from main grid at 2 s. Therefore, the power demand for the SMES-battery HESS is the microgrid power demand, which is 334 kW when the microgrid disconnects from the main grid. Figs. 12 and 13 show that the SMES and battery HESS is capable of dealing with the voltage drop and prevents the battery from surge discharging current changes.

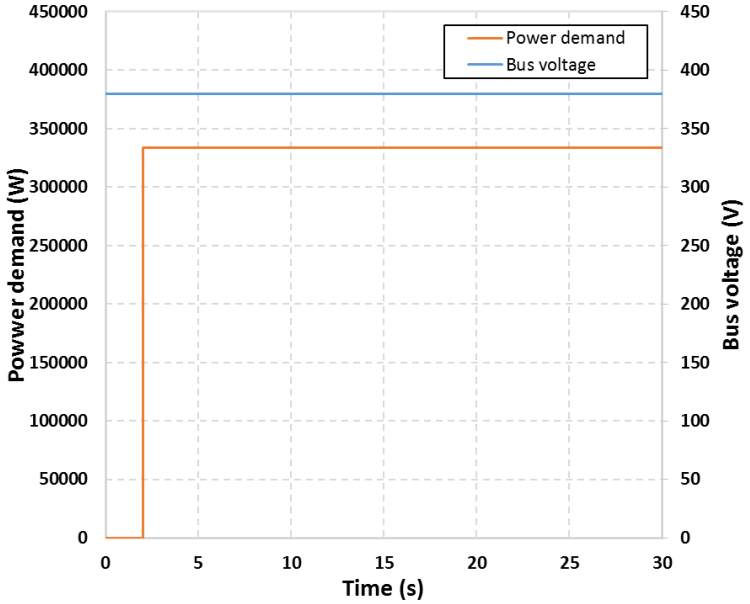

Fig. 12. Power demand and DC bus voltage.

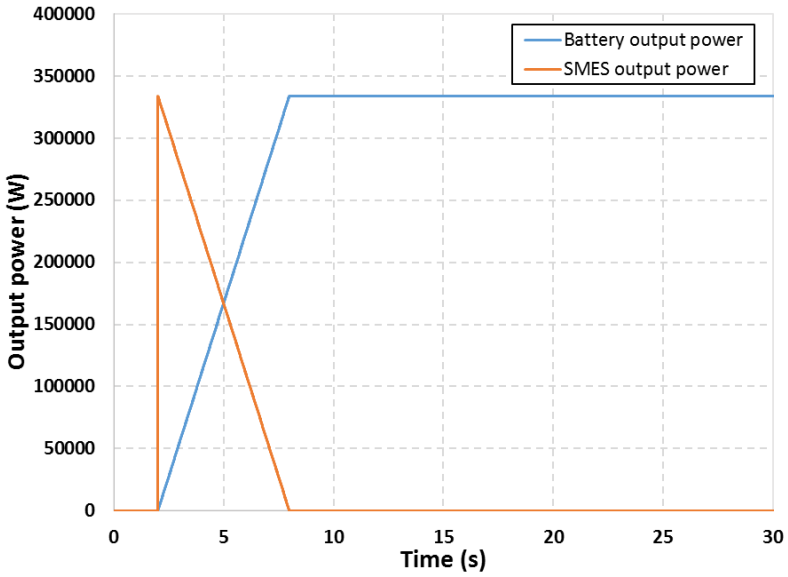

Fig. 13. Simulation results of the SMES and battery power output for a microgrid decoupling application.

As shown in Fig. 13, the battery power output steady rises to the 334 kW, which meets the power demand from the distribution network. The fast responding energy storage device SMES is used to deal with the rest of the power demand before the battery reaches the requested power output. The simulation results match the experimental result, as previously discussed in section 6.

Comparison of the proposed method and the filtration method is shown in Figs. 14 and 15. As the simulation results show the battery power output in Fig 14, the battery power output of the filtration method increases fast when the voltage drop in the microgrid occurs at time 2 s. Furthermore, the battery discharging rate slightly decreases, which makes the battery have a variable discharging rate. The highest discharging rate is uncontrollable and may exceed the battery maximum discharging rate, which means the battery cannot supply enough power to compensate for the power demand. Moreover, for a microgrid application, the filtration method requires higher maximum battery power output. However, the high battery power output will increase the battery attenuation. On the other hand, it may reach, or even exceed, the BESS highest discharging power.

By applying the filtration method, the battery overcharges the system from 8.6 s to 17.2 s. To keep the system stable during this time period, the SMES needs to absorb that amount of energy, as shown in Fig. 15, which is not efficient for the HESS. The filtration method makes the battery, using a longer time, produce the required power output than the proposed PI-droop method. The new proposed method also reduces the battery maximum power output compared with the filtration method. By using the filtration method, the BESS maximum output power requirement reaches 348.4 kW, which is a 4.3% overcharge of the power system's maximum demand. However, the new method does not have overcharge power dealing with the microgrid decoupling process. The over discharge of the HESS to the power system also accelerates the battery lifetime attenuation.

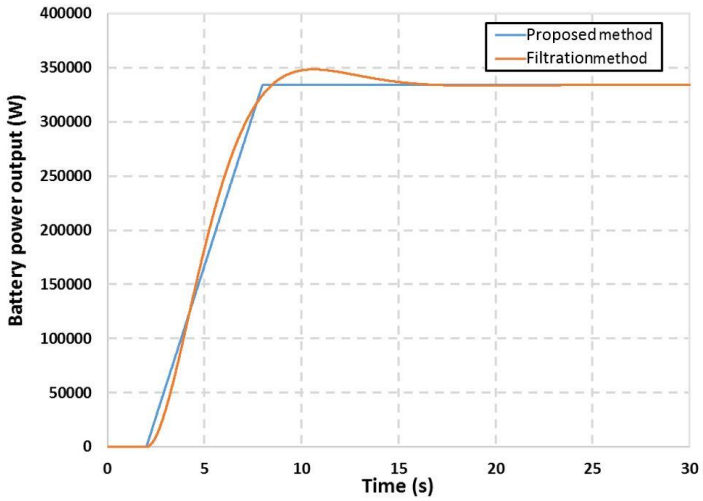

Fig. 14. Battery power output for the filtration control method and the new proposed control method.

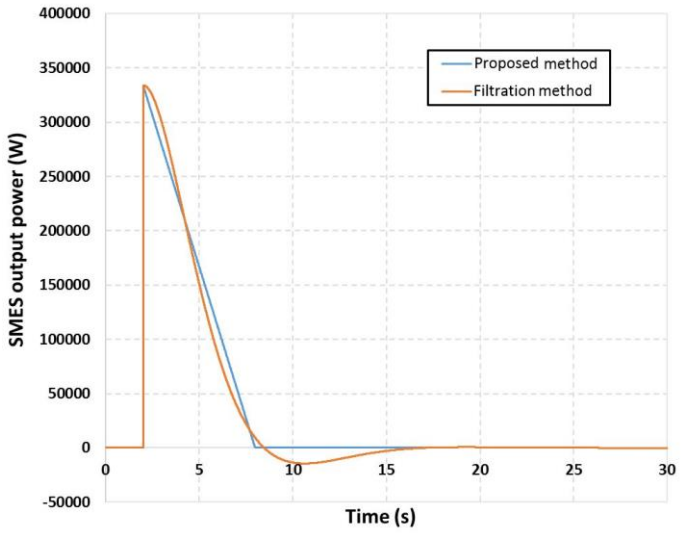

Fig. 15. SMES power output for the filtration control method and the new proposed control method.

As can be seen from Fig. 14, the proposed control method has a fixed battery discharging rate which is 55.8 kW/s. However, the filtration method has a variable discharging rate. Fig. 16 shows the discharging rate for the filtration method. The filtration method has 8.5 s to decrease the power output, which is inappropriate because the system has high power demand from the HESS. The 8.5 s negative discharging rate also shows that the battery has high output power overshoot and needs time to stabilise the battery power output to the expected value. Moreover, as can be seen from Fig. 16, the battery has a higher discharging rate using the filtration control method than the new proposed control method (55.8 kW/s). The battery highest discharging rate for the filtration control method is 78.5 kW/s, which is 141% of the proposed pi-droop control method. The high discharging rate may exceed the BESS maximum discharging rate, which can cause the HESS to be unable to compensate for the power demand in the microgrid. The high discharging rate also accelerates the battery performance attenuation.

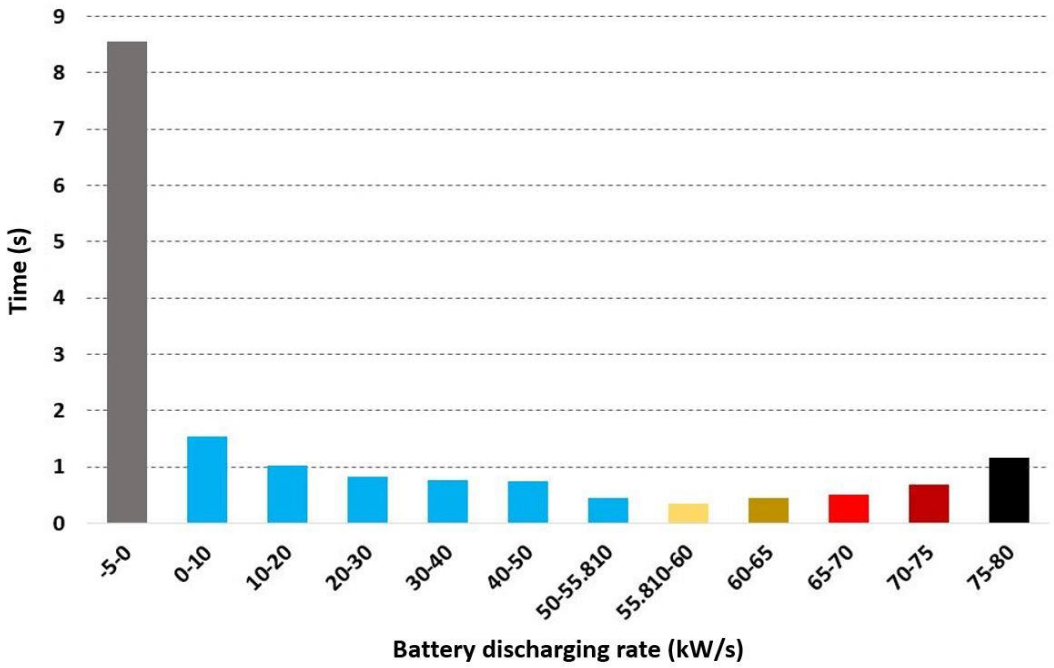

Fig. 16 Discharging rate of the filtration control method applied to the SMES-battery HESS.

The comparison of the discharging rate vs time between the filtration control method and new proposed PI-droop control method is shown in Fig. 17. The filtration method needs 17.05 s to reach the stable battery power output, whilst the proposed method only needs 5.99 s to match the battery output power to the demand power.

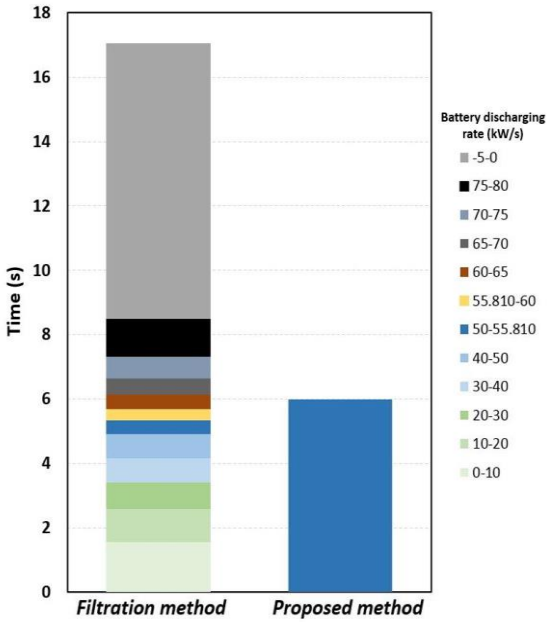

Fig. 17. Discharging rate comparison of the filtration control method and the new proposed PI-droop control method.

Therefore, the new proposed control method has the advantages of high robustness, high reliability and fast response duration, which are necessary to extend the battery service lifetime and compensate for the bus voltage during a microgrid disconnection from the main AC grid.

The battery performance by using two different control methods are summarized in Table 1.

Table 1 Battery performance by using two different control methods

	Two-stage method	Filtration method	Novel two-stage method compared with filtration method
HESS response time until battery reach required power output	5.99 second	17.05 second	Filtration method 185% longer
Battery maximum power output	334 kW	348.435 kW	Filtration method 4.3% higher
Battery maximum discharging changing rate	55.8 kW/s	78.47 kW/s	Filtration method 41% higher

Therefore, according to the study above, the new proposed PI-droop control method has the advantages of high system robustness, high reliability and fast response duration. These advantages are beneficial to extend the battery service lifetime and compensate for the power demand from the microgrid. In this case, the PI-droop method decreases the battery power output by 4.3% and shortens the HESS response speed from 17.05 s to 5.99 s. Moreover, the battery maximum discharging rate decreases by 29%. The low discharging rate and low maximum discharge power helps to extend battery service lifetime. Furthermore, the fast response time helps enhance the system security and reliability.

Another simulation has been done to show the SMES-battery HESS performance when some unexpected load was added to the microgrid, which makes the microgrid power demand higher than the designed power. The proposed method not only needs to control the battery performance but also needs to stabilise the bus voltage. In this situation, a 380 kW power demand is applied for the HESS. The battery maximum discharging power rating for the battery energy storage system is 120 kW/s (in real applications, the discharging rate is much higher than 120 kW/s. In this study, however, the low maximum discharging rate can show the performance of the battery response process when working in stage two). The simulation of the battery power output and SMES power output are shown in Fig. 18.

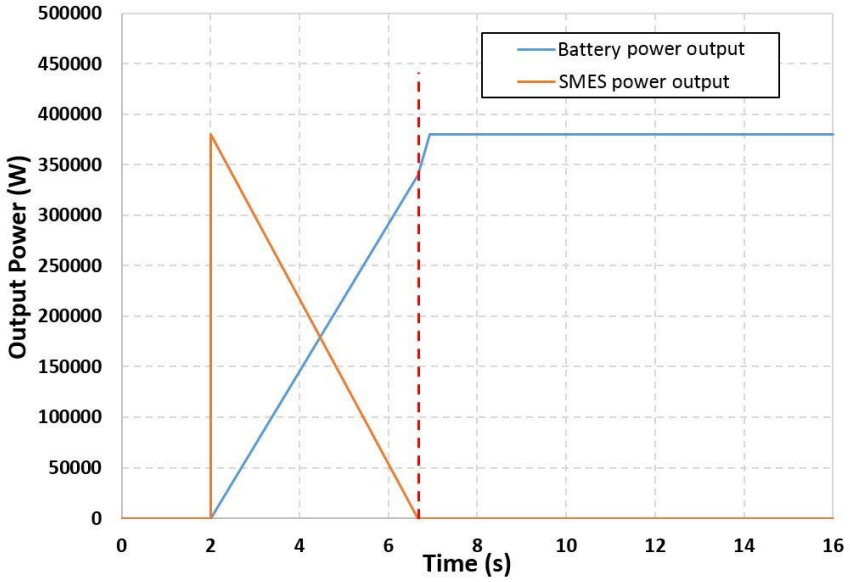

Fig. 18 HESS power output by applying two-stage method for the microgrid with excessive power demand

For case two, when the microgrid switches to isolation mode, stage one starts to operate. The SMES has a high power capacity, which is used to stabilise the power demand to the requested demand. The battery power output is controlled by the stage one control and is working at a 72.85 kW/s discharging rate. At time 6.67 s, the SMES is fully discharged and the battery output power cannot adequately compensate for the power demand from the microgrid. Therefore, stage two starts operating to stabilise the microgrid power demand. From time 6.67 s, the HESS is working in stage two mode, which is the battery DC/DC converter boost mode. The output power is dependent on the battery energy storage system's maximum output power changing rate. The HESS power output reaches 380 kW at 7 s. If the battery energy storage system in the HESS has a higher maximum discharging rate, the battery output power climbing time will become shorter when working with stage two control.

The simulation results of the HESS dealing with an excessive power demand is summarised as Table 2.

Table 2 Simulation result for the microgrid with excessive power demand

Time working at stage one	4.67 s
Time working at stage two	0.33 s
Stage one discharging rate	72.85 kW/s
Stage two discharging rate	120 kW/s
Microgrid voltage unstable time	0.33 s
Maximum power shortage	39.96 kW

The microgrid voltage becomes unstable, which is caused because the HESS not able to deliver enough power to the microgrid. Because the SMES is fully discharged, the SMES cannot support any power output. The battery power output does not reach the required power demand. Therefore, a voltage dip occurs for a short time (0.33 s in this study) until the battery is able to deliver the required power to the system. During the time the HESS is working in stage two, the battery is operating at its maximum discharging rate and trying to meet the microgrid power demand as fast as it can. The maximum power shortage during the microgrid decoupling is 39.96 kW, which is approximately 10% of the overall power demand from the microgrid.

For the same HESS capacity to deal with the excessive power demand, the SMES and battery power output using the filtration method is shown in Fig. 19.

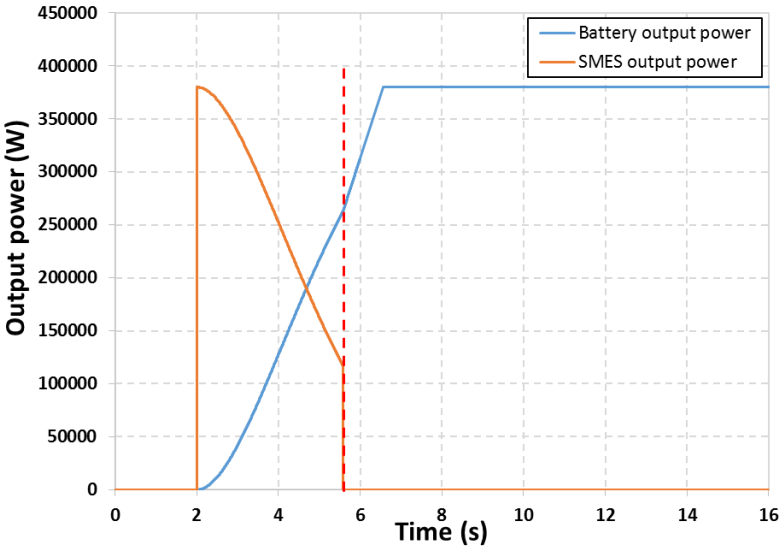

Fig. 19 HESS power output by applying filtration method for the microgrid with excessive power demand

Due to the power demand changes, the filtration method cannot work properly to compensate for the power demand. That is because the cut-off frequency of the filtration control controller is fixed for the normal operating condition and not suitable for different power demands. When the microgrid is disconnected from the main power grid, the HESS, using the filtration method, can keep the voltage stable for the first 3.58 s. However, after the SMES fully discharged, the battery is requested to support all the power demand from the microgrid, which causes the microgrid bus voltage to be unstable for 2.97 s. In this study, the maximum power shortage is 117.16 kW, which is 31% of the microgrid total power demand.

A comparison of the two-stage method and the filtration method are shown in Table 3.

Table 3 Comparison of the two-stage method and filtration method

	Two-stage method	Filtration method
Time duration of battery working at maximum power output	**0.33 second**	**2.97 second**
Maximum microgrid power shortage	**39.96 kW**	**117.16 kW**
Microgrid voltage unstable time	**0.33 second**	**2.97 second**

The filtration method cannot compensate for the microgrid power demand for 2.97 s, which is 791% longer than the proposed two-stage method. Moreover, the higher power shortage of the filtration method can cause a more severe voltage drop in the microgrid. Therefore, the proposed two-stage control method is more suitable for microgrid applications to guarantee microgrid stability and improve battery performance.

As can be seen from the results, the two-stage control method can normally operate to support the microgrid. However, the conventionally used filtration control method is not capable of supporting the demand, which is because the pre-set value does not match the system demand. When an unexpected load added in the system, the conventional control method is not able to support the system with stable voltage. Therefore, the two-stage control method is suitable to enhance the system stability for microgrid applications.

Conclusion:

This paper presents a novel control scheme and sizing design method for a SMES-battery hybrid energy storage system for DC microgrid applications. The proposed control method is able to stabilize the load voltage and manage the SMES and battery power output. An experimental platform was built to test and validate the control methodology and sizing design. The control method for the SMES chopper and battery bidirectional converter has been applied to the experimental platform to test their reliability. The numerical simulation results shows that the proposed novel method makes the battery have better performance for the microgrid coupling and decoupling process compared with a conventional filtration method. Moreover, the proposed control method has a more secure discharging rate, shorter settling time and lower battery output fluctuation.

Appendix:

Table 4 SMES magnet parameters.

Inner radius	45 mm
Outer radius	73 mm
Turn to turn distance	3 mm
Critical current	42 A
Working current	33 A
Inductance	36.65 mH
Number of pancake coils	4

References:

[1] J. M. Guerrero, J. C. Vasquez, J. Matas, L. G. De Vicuña, and M. Castilla, "Hierarchical control of droop-controlled AC and DC microgrids—A general approach toward standardization," *IEEE Transactions on industrial electronics,* vol. 58, pp. 158-172, 2011.

[2] H. Zhou, T. Bhattacharya, D. Tran, T. S. T. Siew, and A. M. Khambadkone, "Composite energy storage system involving battery and ultracapacitor with dynamic energy management in microgrid applications," *IEEE transactions on power electronics,* vol. 26, pp. 923-930, 2011.

[3] C. A. Cortes, S. F. Contreras, and M. Shahidehpour, "Microgrid Topology Planning for Enhancing the Reliability of Active Distribution Networks," *IEEE Transactions on Smart Grid,* 2017.

[4] J. Li, R. Xiong, Q. Yang, F. Liang, M. Zhang, and W. Yuan, "Design/test of a hybrid energy storage system for primary frequency control using a dynamic droop method in an isolated microgrid power system," *Applied Energy,* vol. 201, pp. 257-269, 2017.

[5] H. Kanchev, D. Lu, F. Colas, V. Lazarov, and B. Francois, "Energy management and operational planning of a microgrid with a PV-based active generator for smart grid applications," *IEEE transactions on industrial electronics,* vol. 58, pp. 4583-4592, 2011.

[6] R. Palma-Behnke, C. Benavides, F. Lanas, B. Severino, L. Reyes, J. Llanos*, et al.*, "A microgrid energy management system based on the rolling horizon strategy," *IEEE Transactions on Smart Grid,* vol. 4, pp. 996-1006, 2013.

[7] X. Luo, J. Wang, M. Dooner, and J. Clarke, "Overview of current development in electrical energy storage technologies and the application potential in power system operation," *Applied Energy,* vol. 137, pp. 511-536, 2015.

[8] B. Diouf and R. Pode, "Potential of lithium-ion batteries in renewable energy," *Renewable Energy,* vol. 76, pp. 375-380, 2015.

[9] M. Aneke and M. Wang, "Energy storage technologies and real life applications–A state of the art review," *Applied Energy,* vol. 179, pp. 350-377, 2016.

[10] C. Spanos, D. E. Turney, and V. Fthenakis, "Life-cycle analysis of flow-assisted nickel zinc-, manganese dioxide-, and valve-regulated lead-acid batteries designed for demand-charge reduction," *Renewable and Sustainable Energy Reviews,* vol. 43, pp. 478-494, 2015.

[11] S. P. Ayeng'o, T. Schirmer, K.-P. Kairies, H. Axelsen, and D. U. Sauer, "Comparison of off-grid power supply systems using lead-acid and lithium-ion batteries," *Solar Energy,* vol. 162, pp. 140-152, 2018.

[12] R. Dufo-López, J. M. Lujano-Rojas, and J. L. Bernal-Agustín, "Comparison of different lead–acid battery lifetime prediction models for use in simulation of stand-alone photovoltaic systems," *Applied Energy,* vol. 115, pp. 242-253, 2014.
[13] Q. Long, G. Ma, Q. Xu, C. Ma, J. Nan, A. Li, *et al.*, "Improving the cycle life of lead-acid batteries using three-dimensional reduced graphene oxide under the high-rate partial-state-of-charge condition," *Journal of Power Sources,* vol. 343, pp. 188-196, 2017.
[14] Y. Yuan, C. Sun, M. Li, S. S. Choi, and Q. Li, "Determination of optimal supercapacitor-lead-acid battery energy storage capacity for smoothing wind power using empirical mode decomposition and neural network," *Electric Power Systems Research,* vol. 127, pp. 323-331, 2015.
[15] A. Castaings, W. Lhomme, R. Trigui, and A. Bouscayrol, "Comparison of energy management strategies of a battery/supercapacitors system for electric vehicle under real-time constraints," *Applied Energy,* vol. 163, pp. 190-200, 2016.
[16] M. Farhadi and O. Mohammed, "Energy storage technologies for high-power applications," *IEEE Transactions on Industry Applications,* vol. 52, pp. 1953-1961, 2016.
[17] N. Bizon, "Effective mitigation of the load pulses by controlling the battery/SMES hybrid energy storage system," *Applied energy,* vol. 229, pp. 459-473, 2018.
[18] V. N. Coelho, I. M. Coelho, B. N. Coelho, G. C. de Oliveira, A. C. Barbosa, L. Pereira, *et al.*, "A communitarian microgrid storage planning system inside the scope of a smart city," *Applied Energy,* vol. 201, pp. 371-381, 2017.
[19] Q. Guo, P. Zhang, L. Bo, G. Zeng, D. Li, J. Fan, *et al.*, "An application of high-temperature superconductors YBCO to magnetic separation," *International Journal of Modern Physics B,* vol. 31, p. 1745001, 2017.
[20] A. Ichinose, S. Horii, and T. Doi, "Possibility of material cost reduction toward development of low-cost second-generation superconducting wires," *Japanese Journal of Applied Physics,* vol. 56, p. 103101, 2017.
[21] A. Malozemoff, S. Fleshler, M. Rupich, C. Thieme, X. Li, W. Zhang, *et al.*, "Progress in high temperature superconductor coated conductors and their applications," *Superconductor Science and Technology,* vol. 21, p. 034005, 2008.
[22] W. Yuan, *Second-generation high-temperature superconducting coils and their applications for energy storage*: Springer Science & Business Media, 2011.
[23] J. Li, M. Zhang, Q. Yang, Z. Zhang, and W. Yuan, "SMES/battery hybrid energy storage system for electric buses," *IEEE Transactions on Applied Superconductivity,* vol. 26, pp. 1-5, 2016.
[24] H. Alafnan, M. Zhang, W. Yuan, J. Zhu, J. Li, M. Elshiekh, *et al.*, "Stability Improvement of DC Power Systems in an All-Electric Ship Using Hybrid SMES/Battery," *IEEE Transactions on Applied Superconductivity,* 2018.
[25] J. Li, Q. Yang, F. Robinson, F. Liang, M. Zhang, and W. Yuan, "Design and test of a new droop control algorithm for a SMES/battery hybrid energy storage system," *Energy,* vol. 118, pp. 1110-1122, 2017.
[26] J. Li, Q. Yang, P. Yao, Q. Sun, Z. Zhang, M. Zhang, *et al.*, "A novel use of the hybrid energy storage system for primary frequency control in a microgrid," *Energy Procedia,* vol. 103, pp. 82-87, 2016.
[27] J. Li, X. Wang, Z. Zhang, S. Le Blond, Q. Yang, M. Zhang, *et al.*, "Analysis of a new design of the hybrid energy storage system used in the residential m-CHP systems," *Applied Energy,* vol. 187, pp. 169-179, 2017.
[28] Z. Song, J. Li, X. Han, L. Xu, L. Lu, M. Ouyang, *et al.*, "Multi-objective optimization of a semi-active battery/supercapacitor energy storage system for electric vehicles," *Applied Energy,* vol. 135, pp. 212-224, 2014.
[29] T. Ma, H. Yang, and L. Lu, "Development of hybrid battery–supercapacitor energy storage for remote area renewable energy systems," *Applied Energy,* vol. 153, pp. 56-62, 2015.
[30] T. Ise, M. Kita, and A. Taguchi, "A hybrid energy storage with a SMES and secondary battery," *IEEE Transactions on Applied Superconductivity,* vol. 15, pp. 1915-1918, 2005.
[31] A. M. Gee, F. Robinson, and W. Yuan, "A superconducting magnetic energy storage-emulator/battery supported dynamic voltage restorer," *IEEE Transactions on Energy Conversion,* vol. 32, pp. 55-64, 2017.
[32] B. Meghni, D. Dib, and A. T. Azar, "A second-order sliding mode and fuzzy logic control to optimal energy management in wind turbine with battery storage," *Neural Computing and Applications,* vol. 28, pp. 1417-1434, 2017.
[33] Q. Sun, D. Xing, Q. Yang, H. Zhang, and J. Patel, "A New Design of Fuzzy Logic Control for SMES and Battery Hybrid Storage System," *Energy Procedia,* vol. 105, pp. 4575-4580, 2017.
[34] L. W. Chong, Y. W. Wong, R. K. Rajkumar, and D. Isa, "An optimal control strategy for standalone PV system with Battery-Supercapacitor Hybrid Energy Storage System," *Journal of Power Sources,* vol. 331, pp. 553-565, 2016.
[35] J. G. de Matos, F. S. e Silva, and L. A. d. S. Ribeiro, "Power control in ac isolated microgrids with renewable energy sources and energy storage systems," *IEEE Transactions on Industrial Electronics,* vol. 62, pp. 3490-3498, 2015.
[36] O. Salari, K. H. Zaad, A. Bakhshai, and P. Jain, "Filter Design for Energy Management Control of Hybrid Energy Storage Systems in Electric Vehicles," in *2018 9th IEEE International Symposium on Power Electronics for Distributed Generation Systems (PEDG)*, 2018, pp. 1-7.
[37] A.-L. Allègre, A. Bouscayrol, and R. Trigui, "Flexible real-time control of a hybrid energy storage system for electric vehicles," *IET Electrical Systems in Transportation,* vol. 3, pp. 79-85, 2013.
[38] Z. Song, H. Hofmann, J. Li, X. Han, and M. Ouyang, "Optimization for a hybrid energy storage system in e lectric vehicles using dynamic programing approach," *Applied Energy,* vol. 139, pp. 151-162, 2015.
[39] B. Hredzak, V. G. Agelidis, and M. Jang, "A model predictive control system for a hybrid battery-ultracapacitor power source," *IEEE Transactions on Power Electronics,* vol. 29, pp. 1469-1479, 2014.
[40] Y. Cui, C. Du, G. Yin, Y. Gao, L. Zhang, T. Guan, *et al.*, "Multi-stress factor model for cycle lifetime prediction of lithium ion batteries with shallow-depth discharge," *Journal of Power Sources,* vol. 279, pp. 123-132, 2015.
[41] R. Xiong, L. Li, Z. Li, Q. Yu, and H. Mu, "An electrochemical model based degradation state identification method of Lithium-ion battery for all-climate electric vehicles application," *Applied Energy,* vol. 219, pp. 264-275, 2018.
[42] S. Panchal, I. Dincer, M. Agelin-Chaab, R. Fraser, and M. Fowler, "Thermal modeling and validation of temperature distributions in a prismatic lithium-ion battery at different discharge rates and varying boundary conditions," *Applied Thermal Engineering,* vol. 96, pp. 190-199, 2016.
[43] A. S. Mir and N. Senroy, "Adaptive model predictive control scheme for application of SMES for load frequency control," *IEEE Transactions on Power Systems,* 2017.
[44] J. Hou, J. Sun, and H. Hofmann, "Control development and performance evaluation for battery/flywheel hybrid energy storage solutions to mitigate load fluctuations in all-electric ship propulsion systems," *Applied Energy,* vol. 212, pp. 919-930, 2018.

[45] C. Wang, R. Xiong, H. He, X. Ding, and W. Shen, "Efficiency analysis of a bidirectional DC/DC converter in a hybrid energy storage system for plug-in hybrid electric vehicles," *Applied energy,* vol. 183, pp. 612-622, 2016.
[46] S. Adhikari, Z. Lei, W. Peng, and Y. Tang, "A battery/supercapacitor hybrid energy storage system for DC microgrids," in *Power Electronics and Motion Control Conference (IPEMC-ECCE Asia), 2016 IEEE 8th International*, 2016, pp. 1747-1753.
[47] C.-L. Nguyen and H.-H. Lee, "An optimal hybrid supercapacitor and battery energy storage system in wind power application," in *Industrial Electronics Society, IECON 2015-41st Annual Conference of the IEEE*, 2015, pp. 003010-003015.
[48] H. Alafnan, M. Zhang, W. Yuan, J. Zhu, J. Li, M. Elshiekh*, et al.*, "Stability Improvement of DC Power Systems in an All-Electric Ship Using Hybrid SMES/Battery," *IEEE Transactions on Applied Superconductivity,* vol. 28, pp. 1-6, 2018.
[49] L. Chen, H. Chen, Y. Li, G. Li, J. Yang, X. Liu, *et al.*, "SMES-Battery Energy Storage System for the Stabilization of a Photovoltaic-Based Microgrid," *IEEE Transactions on Applied Superconductivity,* vol. 28, pp. 1-7, 2018.
[50] J. Li, A. M. Gee, M. Zhang, and W. Yuan, "Analysis of battery lifetime extension in a SMES-battery hybrid energy storage system using a novel battery lifetime model," *Energy,* vol. 86, pp. 175-185, 2015.
[51] R. Xiong, Y. Duan, J. Cao, and Q. Yu, "Battery and ultracapacitor in-the-loop approach to validate a real-time power management method for an all-climate electric vehicle," *Applied Energy,* vol. 217, pp. 153-165, 2018.
[52] J. Shen, S. Dusmez, and A. Khaligh, "Optimization of sizing and battery cycle life in battery/ultracapacitor hybrid energy storage systems for electric vehicle applications," *IEEE Transactions on industrial informatics,* vol. 10, pp. 2112-2121, 2014.